5436 *J. Phys. Chem. A* **2008,** *112,* 5436–5447

Two-Way Effects between Hydrogen Bond and Intramolecular Resonance Effect: An Ab Initio Study on Complexes of Formamide and Its Derivatives with Water

Tao Liu,[†] Hua Li,[†] Ming-Bao Huang,[†,*] Yong Duan,[‡,*] and Zhi-Xiang Wang[†,*]

College of Chemistry and Chemical Engineering, Graduate University of Chinese Academy of Sciences, Beijing 100049, P. R. China, and Genome Center, University of California, Davis, California 95616

Received: December 24, 2007; Revised Manuscript Received: April 7, 2008

Ab initio calculations up to MP2/aug-cc-pVTZ//MP2/cc-pVTZ level, including natural charge population and natural resonance theory analyses, have been carried out to study the two-way effects between hydrogen bond (H-bond) and the intramolecular resonance effect by using the H-bonded complexes of formamide (**FAO**) and its derivatives (**FAXs**, **X** represents the heavy atoms in the substituent groups, $=CH_2$, $=NH$, $=SiH_2$, $=PH$, and $=S$) with water as models. Unlike NH_3 and NH_2CH_3 which prefer being H-bond acceptors (**HA**) to form H-bond with water, the amino groups in the six monomers, because of the resonance effect, prefer being H-bond donors (**HD**) rather **HA**. Six monomers can all form **HD** complexes with water, and only two (**FAC** and **FASi**) with the weakest resonance effect are able to form **HA** complexes with water. The **HD** H-bond and resonance effect enhance each other (positive two-way effects) whereas the **HA** H-bond and resonance effect weaken each other (negative two-way effects). The H-bond energies in the six **HD** complexes are nearly linearly correlated with the weights of the dipolar resonance in Pauling's model and the N−C bond lengths; the correlation coefficients are 0.91 and 0.93, respectively. The positive two-way effects also happens in **FAO**−water complex, in which the **FAO** CO group serves as **HA** ($\mathbf{HA_{co}}$). Interestingly, when the **HD** and $\mathbf{HA_{co}}$ H-bonds are present in **FAO** H-bond complex simultaneously, the enhancements are much more significant, and the energies of the two types of H-bonds are much larger than those when only one type of H-bond is present, reflecting the cooperative effects. By using the knowledge to the two-way effects, we computationally designed a molecule ($\mathbf{FAO{-}BH_3}$) to increase H-bond energy. Because of the oxygen lone pair donation to the empty π orbital of BH_3, $\mathbf{FAO{-}BH_3}$ has a much stronger resonance effect than **FAO.** As a result, the H-bond energy (−5.55 kcal/mol) in $\mathbf{HD\ H_2O\cdots FAO{-}BH_3}$ complex is much greater than the −3.30 kcal/mol in the $\mathbf{HD\ H_2O\cdots FAO}$ complex. The two-way effects can be rationalized as follows: the resonance effect leads to intramolecular charge shifts in the monomers which facilitate or prevent the charge donation or acceptation of their H-bond partners. Therefore, the H-bonds are strengthened or weakened. In reverse, the charge donations or acceptations of their H-bond partners facilitate or prevent the intramolecular charge shifts in the monomer moieties, which enhance or weaken the resonance effect. The understanding to the two-way effects may be helpful in drug design and refinement by modulating the H-bond strength and in building empirical H-bond models to study large biological molecules. The study supports Pauling's resonance model.

1. Introduction

The amide linkage (−CO−NH−) is an important functional group in chemistry, biochemistry, and materials science.[1,2] Its dual ability to function as both hydrogen bond (H-bond) donor and acceptor makes the linkage versatile in molecular assembly and recognition. For examples, the H-bonds among peptide bonds in proteins are the key driving forces for forming organized α-helix and *β*-sheet secondary structures. The linkage also plays important roles in the pharmacophores of the antibacterial agents such as penicillins and carbacephems and has been utilized in designing enzyme inhibitors.[1–4]

The ubiquitous nature and the somewhat peculiar planar geometry of the linkage have attracted a wide interest to characterize its fundamental properties. Efforts have been made to understand the prototype of the linkage, the formamide (H_2NCOH, **FAO**), and its derivatives. The planarity of the molecule and the unexpected large internal rotation barrier around N−C bond are the subjects of these studies.[5–29] The rationalization of the phenomena has been the topics of debates.[28–38] Although Pauling's resonance interpretation[38] via the resonances I and II (Scheme 1) has been widely accepted,[28–33] the atoms in molecules (AIM) charge analyses[34–37] suggested that the resonance III may play a more important role than II in formamide and resonance II is significant only in thioformamide. However, the natural resonance theory (NRT), the natural population analysis (NPA),[30] valence-bond (VB)[31,33] and Block-

SCHEME 1

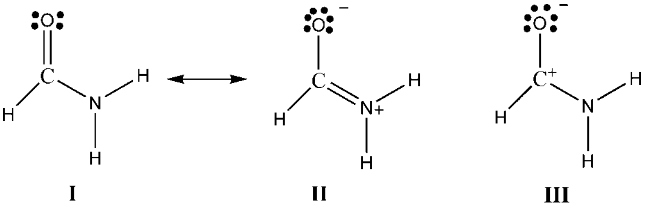

---

* To whom correspondence should be addressed: E-mail: zxwang@gucas.ac.cn (Z.X.W.), duan@ucdavis.edu (Y.D.), and mbhuang1@gucas.ac.cn.

[†] Graduate University of Chinese Academy of Science.

[‡] University of California.

10.1021/jp712052e CCC: $40.75

TABLE 1: Comparison of the Geometrical Parameters of Formamide, Optimized at MP2 and B3LYP Levels with Various Basis Sets, with the CCSD(T)/aug-cc-pVTZ and Experimental Ones

	R(C−N)	R(N−Hs)	R(N−Ha)	R(C=O)	$\angle CNH_s$	$\angle CNH_a$	$\angle H_aNCH_s$
MP2/6-31G**	1.3620	1.0058	1.0035	1.2241	118.5	121.3	168.4
MP2/6-311+G**	1.3689	1.0097	1.0074	1.2163	117.5	119.2	153.4
MP2/cc-pVTZ	1.3576	1.0042	1.0015	1.2150	119.2	121.1	179.8
B3LYP/6-31G**	1.3613	1.0093	1.0071	1.2162	119.0	121.7	180.0
B3LYP /6-311+G**	1.3609	1.0092	1.0067	1.2117	119.4	121.4	180.0
B3LYP /cc-pVTZ	1.3571	1.0063	1.0037	1.2096	119.4	121.4	180.0
CCSD(T)/aug-cc-pVTZ[29]	1.3565	1.0036	1.0012	1.2120	121.1	119.3	180.0
expt[11]	1.352	1.002	1.002	1.219	118.5	120.0	180.0

Localized Wave (BLW) function[31,32] studies, and high-level electron correlation calculations[28,29] provided no evidence to doubt Pauling's resonance model.[38] Although the charge population is defined with a certain arbitrariness and NPA and AIM give distinct representations on the charge density shifts due to the resonance effect, Glendening and Hrabal[30] argued that an orbital-based NPA analysis may be more appropriate than a coordinate-based AIM analysis because the charge shifts given by NPA are essentially consistent with those anticipated from conventional resonance theory and chemical intuition, whereas AIM analysis gives a largely contrasting view.

It is the capability of the linkage to serve as both H-bond donor and acceptor that makes it important in chemistry, biochemistry, and materials science.[1,2] Although the previous studies[5–38] focused on the geometrical and electronic structures of formamide and its derivatives and the debate on the resonance model may continue, the present work is to study the two-way effects between H-bonding and the intramolecular resonance effect. We focus on how substitutions influence the resonance effect and consequently the capability to form H-bond and, in reverse, how the formed H-bond affects the geometrical and electronic structures (i.e., the resonance effect). It should be clarified that the resonance effect we mentioned is intramolecular as described in Scheme 1 rather than intermolecular as in the resonance assisted H-bond (RAHB, D−H···A ↔ D···H−A).[39,40] Furthermore, according to the classical drug design paradigm,[41,42] the effect of a drug in the human body is a consequence of the molecular recognition between the drug and the biological target. The pharmacological activity of a drug is ultimately determined by the interactions between the drug and its target. H-bond is one of the major forces for the interactions. In the drug optimization process, some of the underlying causes of the structure−activity relationships could be traced to a modulation of the H-bond interactions of the drug with the biological partner. Because the amide linkage is an important building block in drugs, the variations of the H-bond strength may be utilized in the drug design or refinement for improving the specificity and affinity, which is, in part, the motivation of the present study.

To study the two-way effects, we first study the substituent effects on the resonance effect in formamide by replacing the =O in formamide with $=CH_2$, =NH, $=SiH_2$, =PH, and =S. By using water as H-bond probe, we then investigate how the resonance effect affects their capability to form H-bond and how the formed H-bond, in reverse, influences the resonance effect. For clarity, the monomers are designated as **FAX** with X (X = C, N, O, Si, P, and S) representing the heavy atoms in the substituent groups.

2. Computational Methods

All structures in this work were fully optimized at the MP2 level with basis sets, 6-31G**, 6-311+G**, and cc-pVTZ and characterized to be minima (no imaginary frequency) by frequency analyses at the MP2/6-31G** level. The H-bond energies used in the discussions were calculated with eq 1

$$\Delta E_{\text{H-bond}} = E_{\text{complex}} - E_{\text{water}} - E_{\text{FAX}} + \Delta E_{\text{BSSE}} + \Delta E_{\text{ZPE}} \quad (1)$$

where E_{complex}, E_{water}, and E_{FAX} are the MP2/aug-cc-pVTZ//MP2/cc-pVTZ single-point energies of the H-bonded complex, water, and **FAX** with X (X = C, N, O, Si, P, and S), respectively. ΔE_{BSSE} is the basis set superposition error (BSSE) correction estimated at the same level by using the standard counterpoise method[43] implemented in Gaussian 03.[44] and ΔE_{ZPE} is the zero-point energy (ZPE) correction at the MP2/6-31G** level.

The previous studies[26,45] have shown that the planarity of formamide is senstitive to the theories and the basis sets used. To validate the present theoretical levels, we compared the optimized geometries of formamide with the availabe high-level (CCSD(T)/aug-cc-pVTZ) theoretical[29] and experimental[11] structures (Table 1). Whereas the MP2/6-31G** and MP2/6-311+G** optimizations were not able to give planar structures, the MP2/cc-pVTZ optimization gave a geometry nearly idential to that of the CCSD(T)/aug-cc-pVTZ[29] and close to the experimental ones.[11] The comparison indicates the reliability of the MP2/cc-pVTZ level in describing this class of compounds. The H-bond energy (−3.97 kcal/mol) of $NH_3\cdots H_2O$ complex, calculated with eq 1, is also very close to the −3.91 kcal/mol at the CCSD(T)/aug-cc-pVTZ//MP2/cc-pVTZ level, which gives us confidence to assume that the level used at least gives reliable trend about H-bond energies although the electron correlations were only accounted at the MP2 level. Although the geometries (Table 1) optimized at the B3LYP level with various basis sets are also in good agreement with the experimental and CCSD(T) ones, the dubious reliability of the DFT method to account for nonbonding energy[46–48] prevents us from using this method in this work. The MP2/cc-pVTZ geometries and the energies based on eq 1 are used in the following discussions.

The NPA,[49–51] NRT,[52–54] and WBI (Wiberg Bond Index)[55] performed at the MP2/aug-cc-pVTZ//MP2/cc-pVTZ level with the MP2 wave functions were used to characterize the electronic structures of the monomers and the H-bonded complexes. All calculations were carried out by using Gaussian 03 program,[44] and the NPA, NRT, and WBI were performed with NBO 5.0 package.[56]

3. Results and Discussion

3.1. Substituent Effects on the Geometries and Resonance Effect of the Monomers. The MP2/cc-pVTZ structures of the six monomers are displayed in Figure 1A. The dihedral angles ($\angle H_aNCH_s$) measure the degree of the planarity of the amino groups. As X atom moves from the left to the right along either

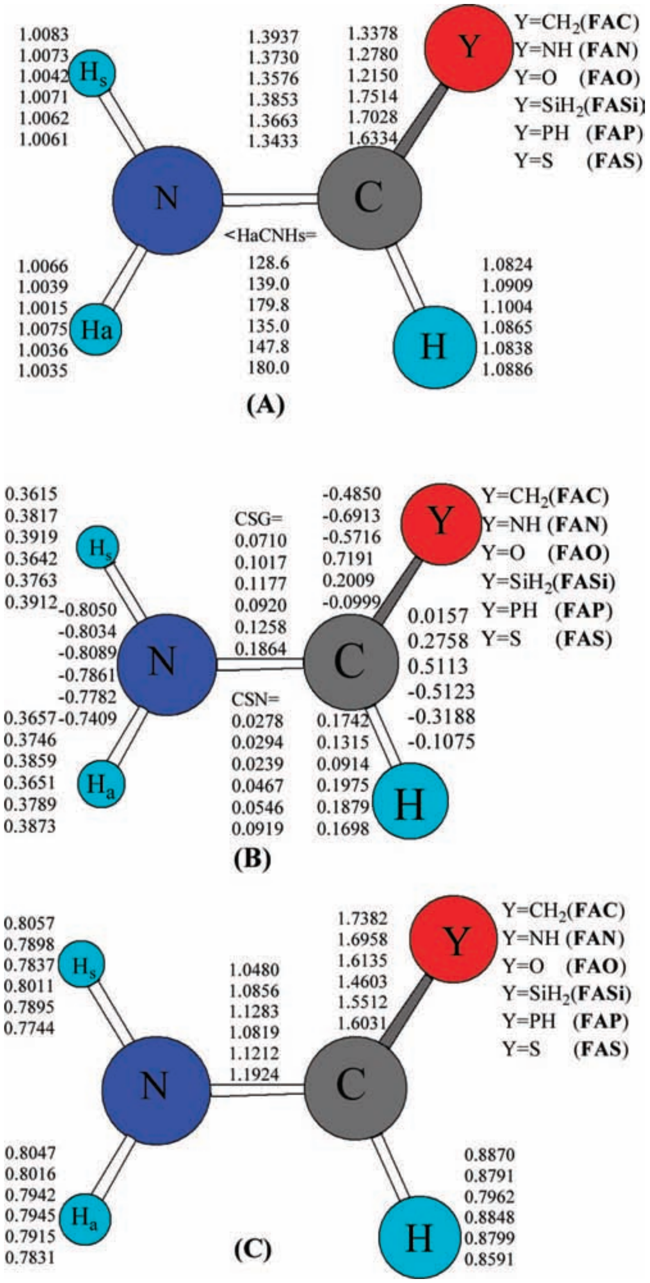

Figure 1. (A) MP2/cc-pVTZ geometries of **FAX** (X = C, N, O, Si, P, and S), including the bond lengths in angstroms and the ∠H_aCNH_s dihedral angles in degrees. (B) MP2/aug-cc-pVTZ//MP2/cc-pVTZ natural charges (in e) of individual atoms and charge shifts relative to the reference (methylamine) on N atoms (CSN) and amino groups (CSG). (C) MP2/aug-cc-pVTZ WBIs.

TABLE 2: Weights of Resonances I, II, and III in Scheme 1 at MP2/aug-cc-pVTZ//MP2/cc-pVTZ Level by NRT with those by VB[31]

	FAC	FAN	FAO	FASi	FAP	FAS	FAC-HD	FAN-HD
I	77.6	73.3	59.0	72.5	65.6	57.2	76.4	63.4
I (VB)[a]	61.1 (72.5)	54.5 (67.7)	46.1 (60.1)					
II	8.2	10.6	27.3	10.8	20.0	29.4	9.1	20.6
II(VB)[a]	19.0 (19.6)	24.6 (26.8)	31.8 (36.6)					
III	2.8	3.3	3.5	2.1	2.0	2.9	2.5	2.5
others	11.4	12.8	10.2	14.6	12.4	10.5	12.0	13.5

	FAO-HD	FASi-HD	FAP-HD	FAS-HD	FAC-HA	FASi-HA	FAO-HA_{CO}
I	56.8	67.7	62.5	54.2	77.0	74.5	56.2
II	28.5	14.0	23.6	31.4	6.0	6.8	29.1
III	3.4	2.5	1.8	2.8	2.8	3.2	2.9
others	11.3	15.8	12.1	11.6	14.2	15.5	11.8

	HD-FAO-HA_{CO}	FAO−BH_3	HD-FAO−BH_3	FAO−Li^+	HD-FAO−Li^+
I	47.8	43.7	41.0	43.5	39.8
II	36.9	37.2	38.7	43.4[b]	45.4[b]
III	2.0	0.9	1.0	2.3	2.4
others	13.3	18.2	19.3	10.8	12.4

[a] Weights of resonances I and II are obtained by 6-VB and 3-VB.[31] and values in parentheses are the weights by 3-VB. [b] Sum of the weights of resonances II and II′ in Scheme 2 (see text).

SCHEME 2

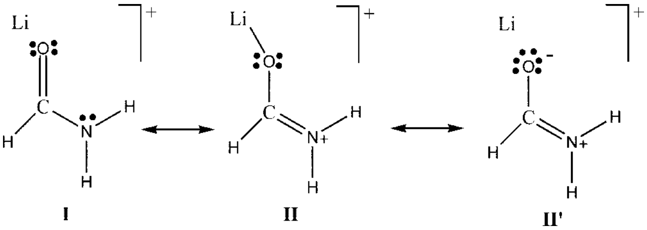

the second or third row in the periodical table, the N−C bond is contracted progressively; the N−C bond lengths in **FAC**, **FAN**, and **FAO** are 1.3937, 1.3730, and 1.3576 Å, respectively, and those in **FASi**, **FAP**, and **FAS** are 1.3853, 1.3663, and 1.3433 Å, respectively. All values are substantially smaller than the standard single N−C bond length (1.4626 Å) in NH_2CH_3. The hybridization difference of carbon in **FAX** (sp^2) and NH_2CH_3 (sp^3) may also contribute the bond length shortening, but the effect due to the hybridization change may be insignificant. For examples, by using the BLW method, Mo and Schleyer[57] estimated that the C(sp^2)−C(sp^2) single bond lengths in benzene Kekule structure, *cis*-butadiene, and *trans*-butadiene are 1.522, 1.529, and 1.517 Å, respectively, in comparison with the standard C(sp^3)−C(sp^3) single bond length (1.526 Å) in ethane. Furthermore, the experimental C−H bond lengths[58] in ethane (1.096 Å), ethene (1.085 Å), and ethyne (1.061 Å) also show small variations due to hybridization change. The apparent shortening of the N−C bond indicates the double bond character of N−C bonds in the monomers and is in agreement with Pauling's resonance model[38] (see below for NRT analyses) shown in Scheme 1, and the increase in the electronegativity of X atom enhances the resonance effect. However, the N−C bonds in **FASi, FAP,** and **FAS** are shorter than those in their second-row counterparts even though the X atoms are less electronegative than their second-row counterparts. The phenomenon has been ascribed to the larger size (polarizability) of the third-row atoms compared to their second-row counterparts,[32] which facilitates the accommodation of the charges shifted from nitrogen because of the resonance effect. Apparently, there is a competition between electronegativity and size effects. As a consequence, the N−C bond in **FAO** is shorter than those in **FASi** and **FAP** despite the large size of Si and P atoms, and the N−C bond in **FAS** is shorter than those in **FAN** and **FAO** despite the large electronegativities of N and O.

The resonance effect lengthens the C=X bond but to a smaller degree than the N−C bond contraction. In their study,[35] Wiberg and Breneman found that as the N−C bond is shortened by 0.08 Å relative to that in the 90°-rotated formamide (in which the resonance effect is assumed to be turned off [23,31] because the nitrogen lone pair is perpendicular to the C=O π component), the C−O bond is elongated only by 0.01 Å, which let Wiberg and Breneman[35] reason an implication of problems in

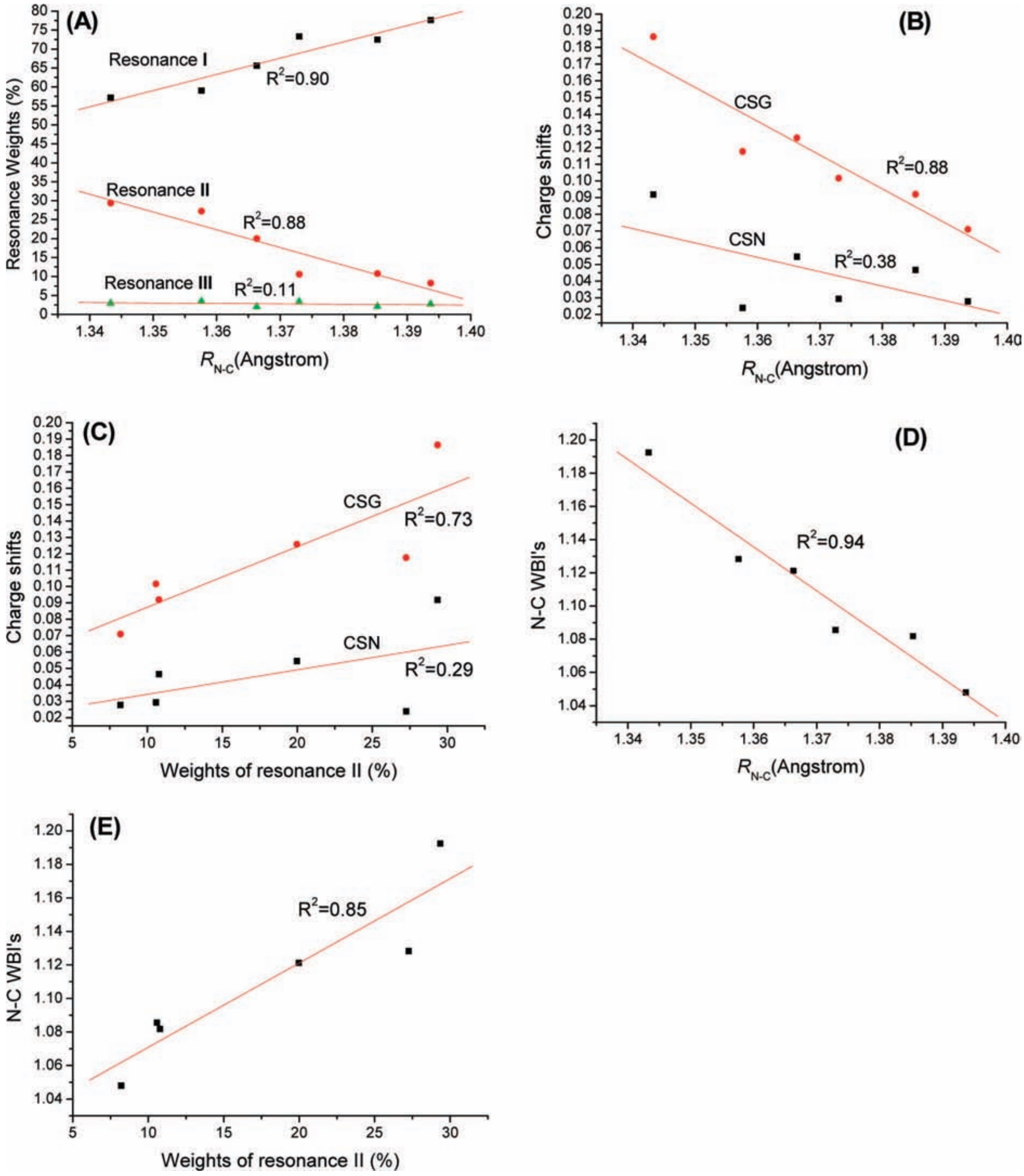

Figure 2. Various correlations among the N−C bond lengths, the weights of resonances, charge shifts, and WBI's for the isolated monomers.

the Pauling's resonance model.[38] It should be pointed that in the 90°-rotated **FAO**, the resonance effect is not completely turned off, and the NRT analyses by Glendening and Hrabal[30] showed that the weights of resonance II in the planar and 90°-rotated **FAO** are 28.6% and 7.8%, respectively, in agreement with Mo and Schleyer's VB study[31] which showed that positive and negative hyperconjugation interactions are predominant in 90°-rotated **FAO.** Both hyperconjugations also contribute to the variations of the N−C and C═O bonds. To investigate this, we used **FAO** as an example and calculated the two-dimensional energy surface around its equilibrium structure at the MP2/aug-cc-pVTZ//MP2/cc-pVTZ level by using N−C and C−O bonds as reaction coordinates. The potential energy surface, given in the Supporting Information (SI1), was constructed with an interval of 0.05 Å for N−C bond, ranging from 1.30 to 1.60 Å, and a spacing of 0.05 Å for C−O bond, ranging from 1.15 to 1.45 Å. The ellipse energy contour reveals that the energy change is less sensitive to the C−O bond lengthening than to the N−C bond shortening, in agreement with the chemical intuition that the formal C═O double bond is stronger than the formal N−C single bond. Consistently, the elongation of C═X bonds (X = C, N, and O) in the monomers relative to that in CH_2═X, ranging from 0.0028 to 0.0056 Å, is less pronounced than the C═X (X = Si, P, and S) elongation (0.0208−0.0401 Å, relative to the corresponding CH_2═X) in the monomers, in agreement with the fact that the formal C═X (X =C, N, and O) double bonds are stronger than the formal C═X (X = Si, P, and S) double bonds. Monomers **FAO** and **FAS** are perfectly planar, and others are more or less away from a perfect plane. However, in line with the degree of N−C bond

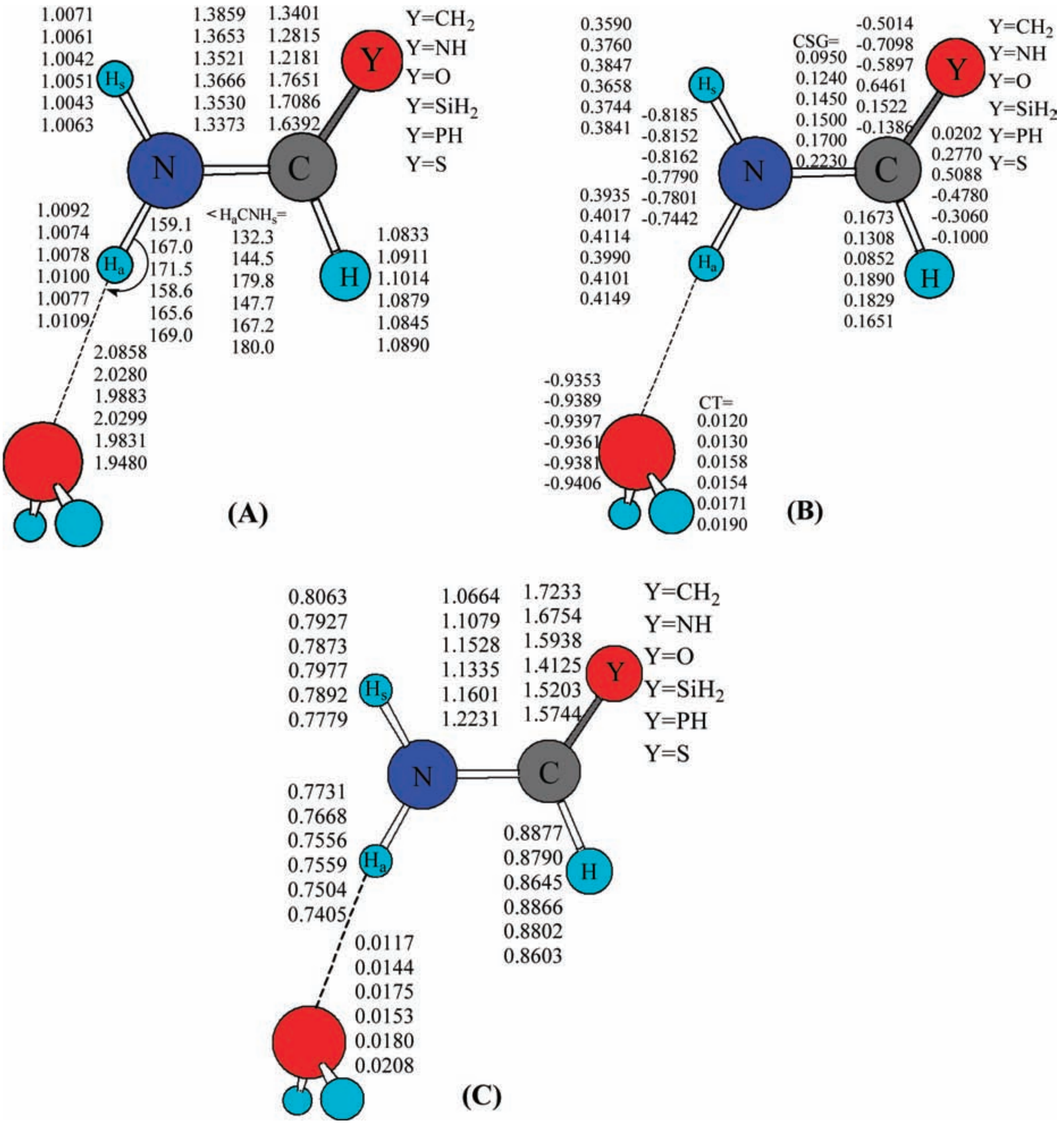

Figure 3. (A) MP2/cc-pVTZ optimized geometries of **FAX-HD** (X = C, N, O, Si, P, and S) complexes, including the bond lengths in angstroms and the $\angle H_aCNH_s$ dihedral angles in degrees. (B) MP2/aug-cc-pVTZ//MP2/cc-pVTZ natural charges (in e) of individual charges and the CT from $NH_2 + H_2O$ groups (CSG). (C) MP2/aug-cc-pVTZ//MP2/cc-pVTZ WBIs.

contraction, the monomers tend to be more planar as the N−C bond is contracted more severely (see Figure 1).

The substituent effects on the geometries are supported by the quantitative NRT analyses. Table 2 lists the weights of the three most predominant resonance structures. In agreement with Pauling's model,[38] resonance I in the six monomers consistently is the most weighted (57.2−77.6%), resonance II ranks second (8.2−29.4%), and resonance III, previously proposed to be important,[35,37] has weights less than 3.5%. The weights of resonances I, II, and III of **FAO** at the current level, 59.0, 27.3, and 3.5%, respectively, are slightly larger those at MP2/6−31+G* level, 58.6, 28.6, and 3.1%, reported by Glendening and Hrabal.[30] Table 2 also includes the weights of the resonances I and II of **FAC**, **FAN**, and **FAO**, given by Mo and Schleyer's VB study.[31] One can note that there are differences among NRT, 6-VB, and 3-VB values, but the three analyses give the same trend, which is that the weight of resonance I decreases and that of resonance II increases as X goes from C to O. By using formaldehyde as a model, Weinhod[59] compared its resonance effect described by NRT analyses at the various theoretical levels (HF, CASSCF, MP2, and B3LYP) and showed that these levels gave similar resonance pictures for the molecule. The previous studies[31,59] indicate that the current method is capable to describe the trend of the series of similar molecules in this study. In the following, the MP2/aug-cc-pVTZ//MP2/cc-pVTZ NRT weights are used.

The correlations between the N−C bond lengths and the weights of resonances I, II, and III are plotted in Figure 2A. Whereas the weights of resonances I and II have strong linear correlations with the N−C bond lengths (correlation coefficients, $R^2 = 0.90$ and 0.88, respectively), there is no correlation between the weights of resonance III and the N−C bond lengths ($R^2 = 0.11$).

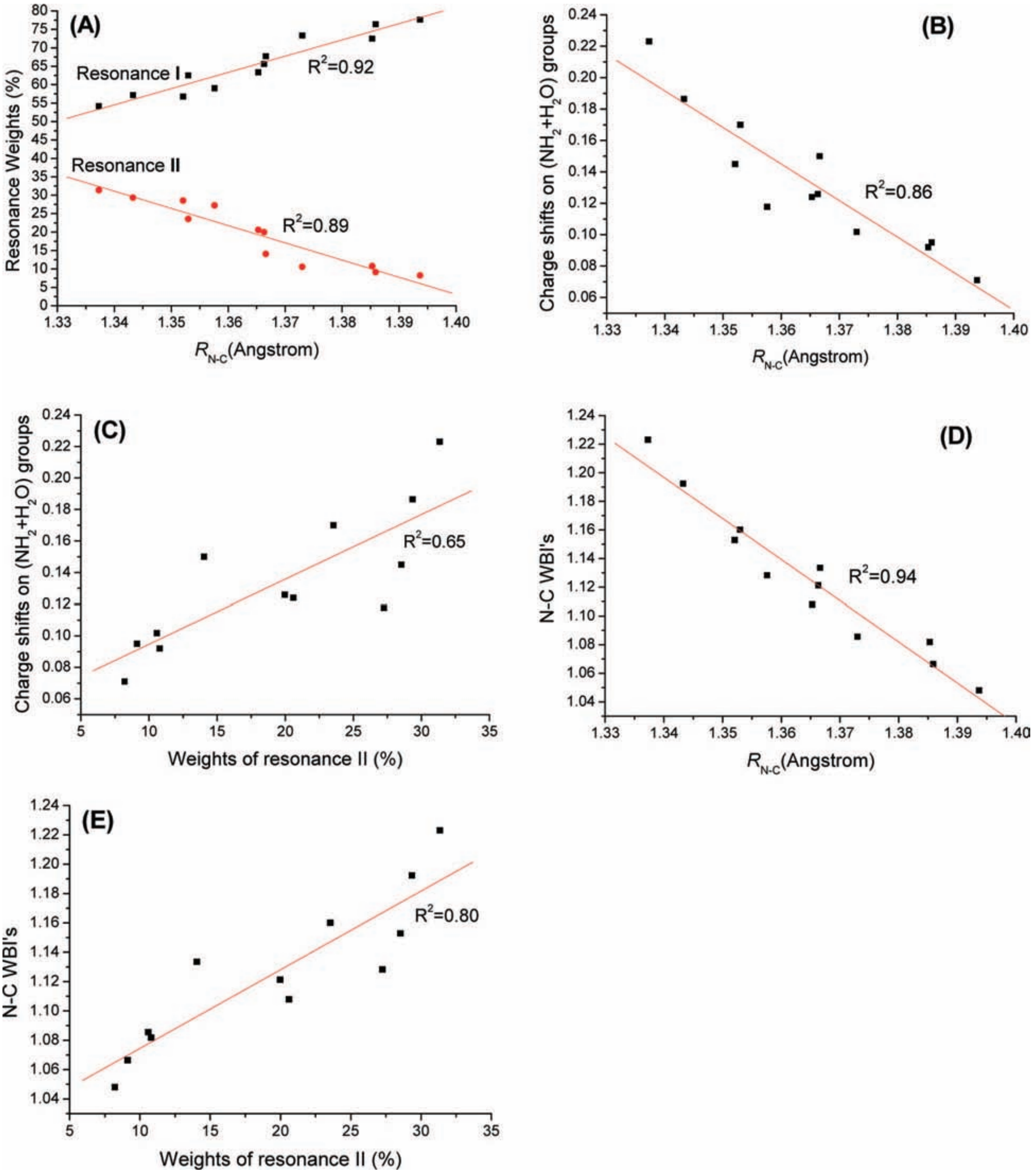

Figure 4. Various correlations among the N−C bond lengths, weights of resonances, charge shifts, and WBIs for the isolated monomers and **FAX-HD** complexes.

Resonance II implies that if the resonance effect is turned off, the amino nitrogen will become more negatively charged and the oxygen will become less negatively charged. The assumption has been studied by rotating the NH_2 group by 90.0° to have the nitrogen lone pair perpendicular to the π component of C═X bond.[28,30–32,35,37] We did not carry out such calculations which focus on one monomer. Instead, we considered the six monomers together and examined the trend of the charge shifts. The charges of the individual atoms, given by NPA analyses, are collected in Figure 1B. In the six monomers, the charges (−0.7409 to −0.8089 e) on nitrogen atoms are all smaller than the −0.8328 e on the nitrogen in NH_2CH_3, which indicates the resonance effect resulting in the charge shifts on nitrogen atoms (CSNs). In the following, we use the charge population of NH_2CH_3 as a reference to discuss the charge shift values. Note that the choice of a reference does not influence the changing trend among the monomers. In agreement with the progressive N−C bond contraction and enhanced role of resonance II, the CSN in the set of **FASi**, **FAP**, and **FAS** increases correspondingly (the CSNs are 0.0467, 0.0546, and 0.0919 e, respectively, relative to the value of −0.8328 e in NH_2CH_3). However, the trend does not hold in the set of **FAC**, **FAN**, and **FAO**; the N−C bond contraction and NRT analyses show that the resonance effect in **FAO** plays more important role than in the other two monomers, but the nitrogen in **FAO** has smaller charge shifts than the other two, the CSNs in **FAC**, **FAN**, and

TABLE 3: H-Bond Energies (in kcal/mol) Calculated at MP2 Level with Various Basis Sets

	MP2					
	6-31G**	6-311+G**	cc-pVTZ	aug-cc-pVTZ[a]	aug-cc-pVTZ[a] + ΔZPE[b]	aug-cc-pVTZ[a] + BSSE[c] + ΔZPE[b]
FAC-HD	−5.35	−4.71	−5.01	−3.50	−2.70	−2.22
FAN-HD	−5.88	−5.36	−5.51	−4.28	−3.38	−2.90
FAO-HD	−6.99	−6.11	−6.43	−4.95	−3.82	−3.30
FASi-HD	−6.62	−5.24	−5.76	−4.01	−3.05	−2.52
FAP-HD	−6.91	−5.83	−6.40	−4.85	−4.04	−3.48
FAS-HD	−7.97	−6.95	−7.27	−5.64	−4.52	−3.95
FAC-HA	−6.84	−6.19	−6.44	−5.15	−3.73	−3.09
FASi-HA	−6.18	−6.17	−6.39	−5.25	−4.33	−3.63
NH_3	−7.92	−7.35	−7.31	−6.23	−4.43	−3.97
NH_2CH_3	−8.66	−8.00	−8.21	−7.16	−5.51	−4.87
FAO-HA$_{CO}$	−8.61	−6.70	−7.69	−6.20	−4.39	−3.76
HD-FAO-HA$_{CO}$	−7.91	−6.92	−7.25	−6.23	−5.01	−4.47
HA$_{CO}$-FAO-HD	−9.53	−7.51	−8.50	−7.36	−5.47	−4.81
H_2CO	−6.83	−5.27	−6.04	−4.80	−2.91	−2.40
HD-FAO-BH_3	−9.84	−8.80	−8.99	−7.20	−6.14	−5.55
HD-FAO-Li^+	−15.52	−13.77	−14.30	−12.21	−10.98	−10.35

[a] MP2/cc-pVTZ geometries were used. [b] ΔZPEs calculated at the MP2/6-31G** level. [c] BSSEs calculated at the MP2/aug-cc-pVTZ//MP2/cc-pVTZ level.

FAO being 0.0278, 0.0294, and 0.0239 e, respectively. Moreover, if considering the six monomers together, one can notice more disagreements between the CSNs and the N−C bond contractions or the weights of resonance II. For example, the nitrogen in **FAO** has smaller charge shifts (0.0239 e) than those in **FASi** (0.0467 e) and **FAP** (0.0546 e), but the former has shorter N−C bond length and larger weight of resonance II than the latter. Figure 2B,C indicates that there is no clear correlation between CSNs and the N−C bond lengths and the weights of resonance II. The correlation coefficients are 0.38 and 0.29, respectively.

The disagreements can be conciliated by considering the total charge shifts on the amino groups (CSGs). Because as the resonance effect occurs, all electrons are reorganized to adapt to the new chemical environment, the hydrogen atoms in amino groups therefore also play a role, and the charge shifts on the amino groups are more informative. By using the total charge (−0.1488 e) on the NH_2 group in NH_2CH_3 as a reference, the CSGs in **FAX** (X = C, N, O, Si, P, and S) are 0.0710, 0.1017, 0.1177, 0.0920, 0.1258, and 0.1864 e, respectively. As shown in Figure 2B,C, the group charge shifts are much better correlated with the N−C bond lengths and the weights of resonance II. The correlation coefficients with the N−C bond lengths and the weights of resonance II are 0.88 and 0.73, respectively. The correlation implies that resonance III plays a limited role in the formamide and its derivatives, because resonance III implies no CSNs or CSGs.

The double-bond character of N−C bonds is also indicated by the WBIs (shown in Figure 1C). The WBIs of N−C bonds in the monomers, ranging from 1.0480 to 1.1924, are larger than the value of 0.9622 in NH_2CH_3. The correlations of the N−C WBIs with N−C bond lengths and the weights of resonance II are plotted in Figure 2D,E, respectively, which shows the good correlations ($R^2 = 0.94$ and 0.85, respectively).

3.2. Two-Way Effects between H-Bond and Resonance Effect. Both ammonia and methylamine (NH_2CH_3) prefer being H-bond acceptors to form stable H-bonded complexes with water. In contrast, the amino groups in the six monomers can all serve as H-bond donors to form stable H-boned complexes, and only two (**FAC** and **FASi**, which have the weakest resonance effect as indicated by the N−C bond contractions and the weights of resonance II) are able to function as H-bond acceptors to form stable H-bonded complexes with water. We designate the two types of H-bonds as **HD** (H-bond donor) and **HA** (H-bond acceptor) and label the corresponding complexes as **FAX-HD** (X = C, N, O, Si, P, and S) and **FAX-HA** (X = C and Si).

3.2.1. Positive Two-Way Effects between* HD *H-Bond and the Resonance Effect. The geometries of the six **HD** complexes are displayed in Figure 3A. Comparison of the geometries of the **FAX** moieties in the complexes with their corresponding monomers (Figure 1A) shows similar trends of N−C bond contraction, C−X bond elongation, and planar deviation to those in the free monomers as X moves across the periodical table. Nevertheless, the H-bonds have an appreciable influence on the geometries of the **FAX** moieties. Relative to the isolated monomers, the N−C bonds are further shortened by 0.0055−0.0187 Å, and the C−X bonds are further elongated by 0.0023−0.0137 Å. The amino groups tend to be more planarized; the $\angle H_aNCH_s$ dihedral angles increase by 3.7−19.4°. **FAO-HD** and **FAS-HD** are exceptions to this because their $\angle H_aNCH_s$ dihedral angles already reach the maximum (180.0°) in the free monomers. The geometrical deviations to the isolated monomers signify that the **HD** H-bond enhances the resonance effect. Intuitively, because the amino groups are **HDs**, there are negative charge transfers (CTs, Figure 3B) from water to the monomers through amino groups. The charge accumulation on the amino groups pushes more negative charges away from the group. Comparing Figure 1B with Figure 3B, one can notice that the charge shifts on $NH_2 + H_2O$ moieties are larger than those in the free monomers. The changes in the geometries are also consistent with the larger weights of resonance II (ca. 0.9−10.0%) and WBIs of N−C bonds in the complexes than those in the corresponding monomers. The N−H_a bond lengthening in the complexes can be interpreted by the electrostatic interaction model,[60–62] according to which the oxygen of water pulls the H-bond proton away from nitrogen, or the hyperconjgation model,[63] which attributes the lengthening to the donation of oxygen lone pair to the N−H antibonding orbital. With respect to the monomer, the N−H_s bond lengths only change marginally.

The correlations described in Figure 2 can even be extended to include the six complexes together. Figure 4A−E shows the various correlations corresponding to Figure 2A−E, respectively. The R^2 values, 0.92, 0.89, 0.86, 0.65, 0.94, and 0.80, are

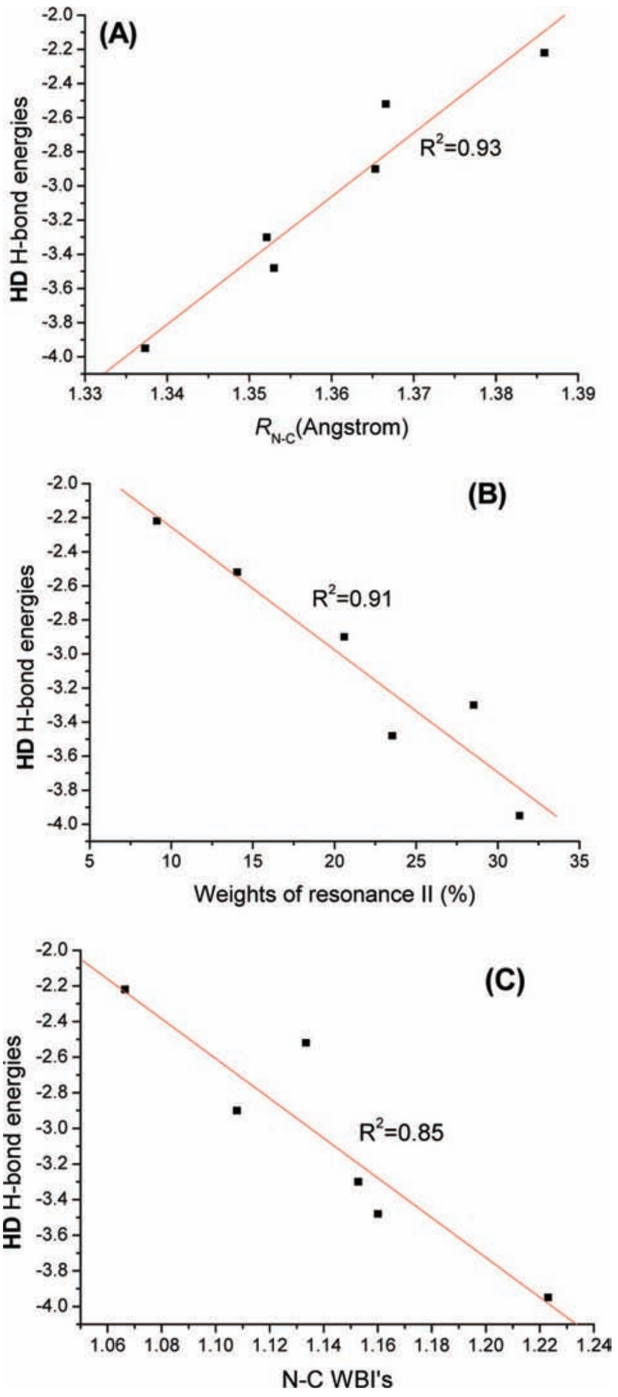

Figure 5. Various correlations among H-bond energies, N−C bond lengths, weights of resonances, and WBIs for the **FAX-HD** complexes.

compared with the values of the monomer case, 0.90, 0.88, 0.88, 0.73, 0.94, and 0.85, respectively.

The H-bonds in **FAX-HD** complexes become increasingly strong as the X atoms become growingly electronegative in the same row of the periodical table. The H-bond energies in **FAC-HD**, **FAN-HD**, and **FAO-HD** (given in Table 3) are −2.22, −2.90, and −3.30 kcal/mol and −2.52, −3.48, and −3.95 kcal/mol in **FASi-HD**, **FAP-HD**, and **FAS-HD**, respectively. The H-bond energies in **FASi-HD**, **FAP-HD**, and **FAS-HD** are larger than their second-row counterparts. As shown by Figure 5A,B,C, the H-bond energies are well correlated with the N−C bond lengths, the weights of resonance II, and the N−C WBIs. The correlations indicate that the resonance effect tends to strengthen the **HD** H-bond.

H-bond interactions are dominated by the electrostatic interactions and the partial covalent bonding because of the CT effect. For the electrostatic contributions, the negative charges on nitrogen atoms are unfavorable for H-bonding because of the Coulomb repulsion between nitrogen and the oxygen of water, which is the partial reason why resonance II (which results in smaller charges on nitrogen) favors the **HD** H-bond. The charges on nitrogen atoms are in qualitative agreement with the H-bond energies. The complexes with the third-row X atoms have larger H-bond energies than those of their counterparts with the second-row X atoms; **FAX-HD** (X = Si, P, and S) have charges on nitrogen atoms of −0.7790, −0.7801, and −0.7442 e, less than those in **FAX-HD** (X = C, N, and O, −0.8185, −0.8152, and −0.8162 e). However, disagreements can also be found. For example, the nitrogen in **FAO-HD** bears larger negative charge (−0.8162 e) than that in **FASi-HD** (−0.7790 e), but the H-bond energy (−3.30 kcal/mol) in **FAO-HD** is larger than that in **FASi-HD** (−2.52 kcal/mol). The disagreements can be attributed to the fact that the electrostatic repulsions are only secondary with respect to the primary electrostatic attractions between water oxygen and the H-bond hydrogen. For the primary electrostatic attractions, the increasing positive charges on H-bond hydrogen atoms (H_a) and increasing negative charges on the water oxygen atoms are consistent with the increasing H-bond energies as X atoms going from the left to the right in either the second or third row. The covalent bonding character of H-bond due to CT is reflected by the WBIs of H-bond and H-bond angles ($\angle OH_aN$). As the X atoms move from the left to the right in either the second or third row, the WBI of H-bond increases, the $\angle OH_aN$ H-bond angle becomes closer to 180.0°, and in the meantime, the $H_a\cdots O$ H-bond lengths decrease (Figure 3A,C).

In short, the resonance effect can enhance the **HD** H-bond through the following effects: (a) reducing the unfavorable repulsion between the amino nitrogen and oxygen of water, (b) enhancing the favorable attraction between the H-bond hydrogen and the **HA** atom, and (c) facilitating the CT from the **HA** to the **HD**. The enhancement of the resonance effect by H-bond is because the charge accumulation on the amino group due to the CT from **HA** pushes more electrons away from the amino group to the other fragments. We refer to the bilateral effects between H-bond and the resonance effect as the two-way effects. Because in the **HD** complexes, the intramolecular resonance effect and the H-bond enhance each other, we call the effects positive two-way effects.

3.2.2. Negative Two-Way Effect between* HA *H-Bond and Resonance Effect. The **HA** H-bond is the prefered pattern in $H_2O\cdots NH_3$ and $H_2O\cdots NH_2CH_3$ complexes. In contrast, only two (**FAC** and **FASi**) of the six monomers are able to form stable **HA** complexes, and the optimization on **FAO**, **FAP**, and **FAS** with initial **HA** H-bond geometries gave **HD** complexes at three optimization levels. For **FAN**, although we could obtain a **HA** complex at lower levels (MP2/6-31G** and MP2/6-311+G**), the optimization at MP2/cc-pVTZ showed that the probe (water) can form two H-bonds simultaneously, one between the oxygen of water and the amino hydrogen and another between the hydrogen of water and the nitrogen in the ═NH substitutent (see Supporting Information, SI2). We reasoned that the nitrogen lone pairs in **FAO**, **FAP**, and **FAS** are so involved in the π conjugation that they lost their capabilities as **HAs**. Consistently, as indicated by the N−C bond lengths and the weights of resonance II, **FAC** and **FASi** monomers have weaker resonance effect than the others. **FAN,** having the weight of resonance II (10.6%) close to that in **FASi**

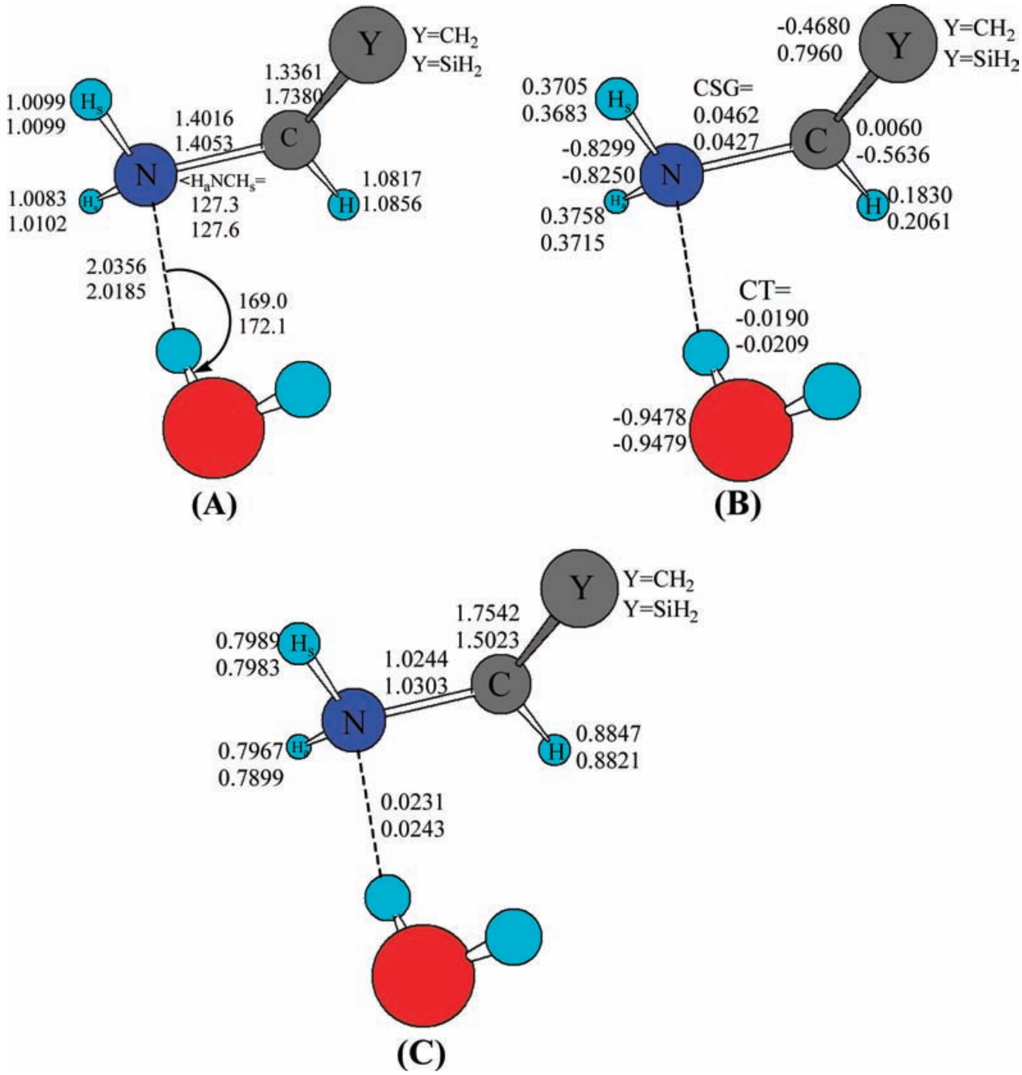

Figure 6. (A) MP2/cc-pVTZ optimized geometries of **FAX-HA** (X = C and Si) complexes, including the bond length in angstroms and the ∠H_aCNH_s dihedral angles in degrees. (B) MP2/aug-cc-pVTZ//MP2/cc-pVTZ natural charges (in e) of individual charges and CT from $NH_2 + H_2O$ groups (CSG). (C) MP2/aug-cc-pVTZ//MP2/cc-pVTZ WBIs.

(10.8%), has the tendency to form **HA** complex, but the nitrogen in the ═NH substitutent prevents it from forming a **HA** complex similar to those of **FAC** and **FASi**.

The geometries of the two **HA** complexes are displayed in Figure 6A. Relative to the free monomers, the N−C bonds in **FAC-HA** and **FASi-HA** are lengthened. Recall that the N−C bonds in the **HD** complexes are shortened. The N−C bond lengths, 1.4016 and 1.4053 Å in **FAC-HA** and **FASi-HA** complexes, respectively, are longer than those (1.3937 and 1.3853 Å) in the **FAC** and **FASi** and those (1.3859 and 1.3666 Å) in **FAC-HD** and **FASi-HD**. The N−C bond elongations are in agreement with the decreased weights of resonance II. The weights of resonance II, 6.0% in **FAC-HA** and 6.8% in **FASi-HA**, are smaller than the values in their free counterparts (8.2 and 10.8%) and the values in the **FAC-HD** and **FASi-HD** complexes (9.1 and 14.0%). However, the N−C bonds in **FAC-HA** and **FASi-HA** are still shorter than the N−C single bond (1.4626 Å) in NH_2CH_3, indicating that the resonance effect is not turned off by the **HA** H-bond completely. Because of the decreased resonance effect, the **FAC** and **FASi** moieties in the two complexes are less planar than the isolated **FAC** and **FASi** monomers and their corresponding **HD** complexes.

The nitrogen atoms in **FAC-HA** and **FASi-HA** are **HAs** and donate negative charges to water molecules, which results in an electron deficiency on nitrogen. The electron deficiency is not favorable for the charge shifts and therefore leads to a weakened resonance effect. Indeed, the charge shifts from $NH_2 + H_2O$ groups in **FAC-HA** and **FASi-HA**, 0.0462 and 0.0427 e, are less than those on NH_2 groups in **FAC** and **FASi** (0.0710 and 0.0920 e) and those of $NH_2 + H_2O$ moieties in **FAC-HD** and **FASi-HD** (0.0950 and 0.1500 e), respectively.

The H-bond lengths in **FAC-HA** and **FASi-HA**, 2.0356 and 2.0185 Å, are shorter than those in **FAC-HD** and **FASi-HD**, 2.0858 and 2.0299 Å, respectively, and the WBIs of H-bonds, 0.0231 and 0.0243, are larger than those in the corresponding **HD** complexes, 0.0117 and 0.0153. Consistently, the H-bond energies in **FAC-HA** (−3.09 kcal/mol) and **FASi-HA** (−3.63 kcal/mol) are larger than those in **FAC-HD** (−2.22 kcal/mol) and **FASi-HD** (−2.52 kcal/mol). Nevertheless, because of the distributions of the resonance effect, the H-bond energies are less than that in the $H_2O\cdots NH_3$ complex (−3.97 kcal/mol) and that in the $H_2O\cdots NH_2-CH_3$ complex (−4.87 kcal/mol). In agreement with the larger H-bond energies in **FAC-HA** and **FASi-HA** than those in **FAC-HD** and **FASi-HD**, the CT amounts between H_2O and monomers in the former, 0.0190 and 0.0209 e, are also larger than those in the latter (0.0120 and 0.0154 e).

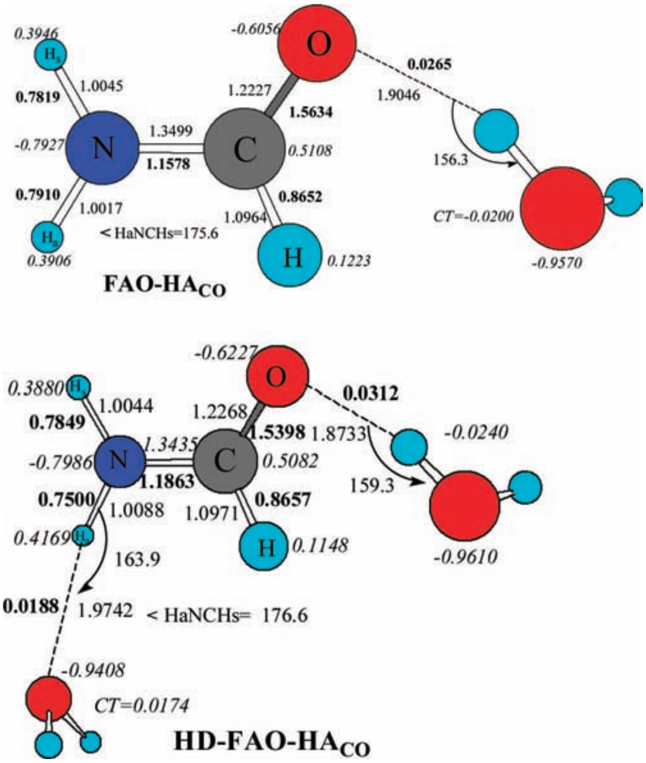

Figure 7. MP2/cc-pVTZ geometries of **FAO-HA$_{co}$** and **HD-FAO-HA$_{co}$** (bond lengths in angstroms, bond and dihedral angles in degrees), MP2/aug-cc-pVTZ//MP2/cc-pvTZ natural charges (in e) in italic, and MP2/aug-cc-pVTZ//MP2/cc-pVTZ WBIs in bold.

In the **HD** complexes, the resonance effect and H-bond enhance each other. In contrast, they weaken each other in the **HA** complexes, to which we refered as the negative two-way effects.

***3.2.3. Positive Two-Way Effects as* FAO *Oxygen Serves as* HA.** In the above discussions, we have only considered the H-bonds using amino groups as **HDs** or **HAs**. The carbonyl group in **FAO** can also function as **HA**. In the H-bonded complex (designated as **FAO-HA$_{co}$**) shown in Figure 7, the N−C bond length (1.3499 Å) is shorter than that in free **FAO** (1.3576 Å) and that in **FAO-HD** (1.3521 Å). Correspondingly, the weight (29.1%) of resonance II in **FAO-HA$_{co}$** is larger than that in **FAO**(27.3%). The enhanced resonance effect can be attributed to the charge donation of the CO group, causing the electron deficiency. The electron deficiency facilitates the charge shifts on amino group. Owing to the enhanced resonance effect, the H-bond energy (−3.76 kcal/mol) in **FAO-HA$_{co}$** is larger than the that in H_2CO•••H_2O complex (−2.40 kcal/mol (Table 3).

We have observed the positive two-way effects between the resonance effect and the **HD-** and **HA$_{co}$** (in **FAO**) H-bond. What are the effects if the two types of H-bonds are present simultaneously as shown in the complex **HD-FAO-HA$_{co}$** (Figure 7)? The NRT analysis revealed that the weight of resonance II in this complex, relative to the **FAO**, is increased by 9.6%. The 9.6% increase of resonance II is significantly larger than the total increase (3.0%) contributed by the individual **HD** and **HA$_{co}$** H-bonds. This reflects the significant cooperative effects, a subject of many studies.[64–77] We here emphasize that the resonance effect can also be affected cooperativly. The **HD** and **HA$_{co}$** H-bond energies in **HD-FAO-HA$_{co}$** are −4.47 and −4.81 kcal/mol, respectively, larger the those in **FAO-HD** (−3.30 kcal/mol) and in **FAO-HA$_{co}$** (−3.76kcal/mol), further indicating the cooperative effects.

3.2.4. Examples to Increase the H-Bond Energy. In drug design and refinement, it is often desirable to increase the H-bond energies to improve the binding affinity (activity) of the drug. The understanding to the two-way effects can help develop a strategy to modulate the H-bond strength. Because the electron donation of carbonyl oxygen in **FAO** can enhance the resonance effect and therefore strengthen the H-bond formed at the amino end, as illustrated in Figure 8, we introduce Lewis acid (e.g., BH_3) to interact with the carbonyl group in **FAO**, giving **FAO-BH$_3$**. The donation of oxygen lone pair to the empty orbital of BH_3, forming a dative O−B bond (WBI_{O-B} = 0.5166 and bonding energy = −18.38 kcal/mol), results in electron deficiency on the carbonyl group, which greatly facilitates the charge shifts from amino group and therefore enhances the resonance effect. The weights of resonance II, 37.2% in **FAO-BH$_3$**, are much larger than those in free **FAO** (27.3%) and in **FAO-HD** complex (28.5%). Consequently, the N−C bond (1.3221 Å) is much shorter than that in **FAO** (1.3576 Å) and that in **FAO-HD** (1.3521 Å). Note that the WBI (1.2798) of N−C bond in **FAO-BH$_3$** is the largest among all compounds reported. The NH_2 group in **FAO** bears a negative charge of −0.0311 e. In contrast, the NH_2 group in **FAO-BH$_3$** has a positive charge (0.1007 e) due to the significant charge shift. The enhanced resonance effect strengthens the **HD** H-bond significantly. The **HD** H-bond energy in the complex **HD···FAO-BH$_3$** (Figure 8), −5.55 kcal/mol, is much larger than that in **FAO-HD** (−3.30 kcal/mol) and even larger than that of the **HD** H-bond in **HD-FAO-HA$_{co}$** (−4.47 kcal/mol). The larger H-bond energy in **HD···FAO-BH$_3$** is also indicated by the shorter H-bond length (1.8943 Å) and larger CT (0.0219 e) and WBI (0.0251) than those in **H$_2$O•••FAO** (1.9833 Å, 0.0158 e, and 0.0175, respectively) and those in **HD-FAO-HA$_{co}$** (1.9742 Å, 0.0174 e, and 0.0188, respectively). Because of the positive two-way effects of the formed **HD** H-bond at the amino group end, the carbonyl group tends to donate more electrons to the BH_3 group; the total atomic charges on the BH_3 group in **FAO-BH$_3$** and **HD-FAO-BH$_3$** are −0.3253 and −0.3358 e, respectively. Consistently, the O−B bond in **HD-FAO-BH$_3$** is stronger than that in **FAO-BH$_3$**, which is reflected by the larger WBI (0.5272) and bonding energy (−20.50 kcal/mol). The weight of resonance II, 38.7%, in **HD-FAO-BH$_3$** is larger than that in **FAO-BH$_3$** 37.2%, in agreement with the above conclusion that **HD** H-bond enhances the resonance effect.

If the modification can be introduced in the drug design or refinement without considering other side effects, the increase (2.25 kcal/mol relative to that in **FAO-HD**) in binding energy can enhance the binding affinity by about 30-fold.

Another extreme example is to use Li^+ as the electron acceptor at the carbonyl end. Because of the severer electron deficiency of Li^+ than that of BH_3, the effect is more pronounced, which is indicated by the even shorter C−N bond length (1.3184 Å) and larger weight of resonance II (43.4%, which is the sum of the weights (33.2 and 10.2%) of the two resonances (II and II′, respectively) shown in Scheme 2). The CT (0.0339 e) in the **HD-FAO-Li$^+$** complex is also larger than that in **HD-FAO-BH$_3$** (0.0219 e). However, the contribution due to the cationic character of the **FAO-Li$^+$** moiety obviously contributes to the very large H-bond energy in **HD-FAO-Li$^+$** (−10.35 kcal/mol). Similar to the first example, the positive two-way effect of **HD** H-bond is also manifested by the shortened N−C bond length and the increased weight of resonance II (see Table 2 and Figure 8) relative to those of monomer **FAO-Li$^+$**.

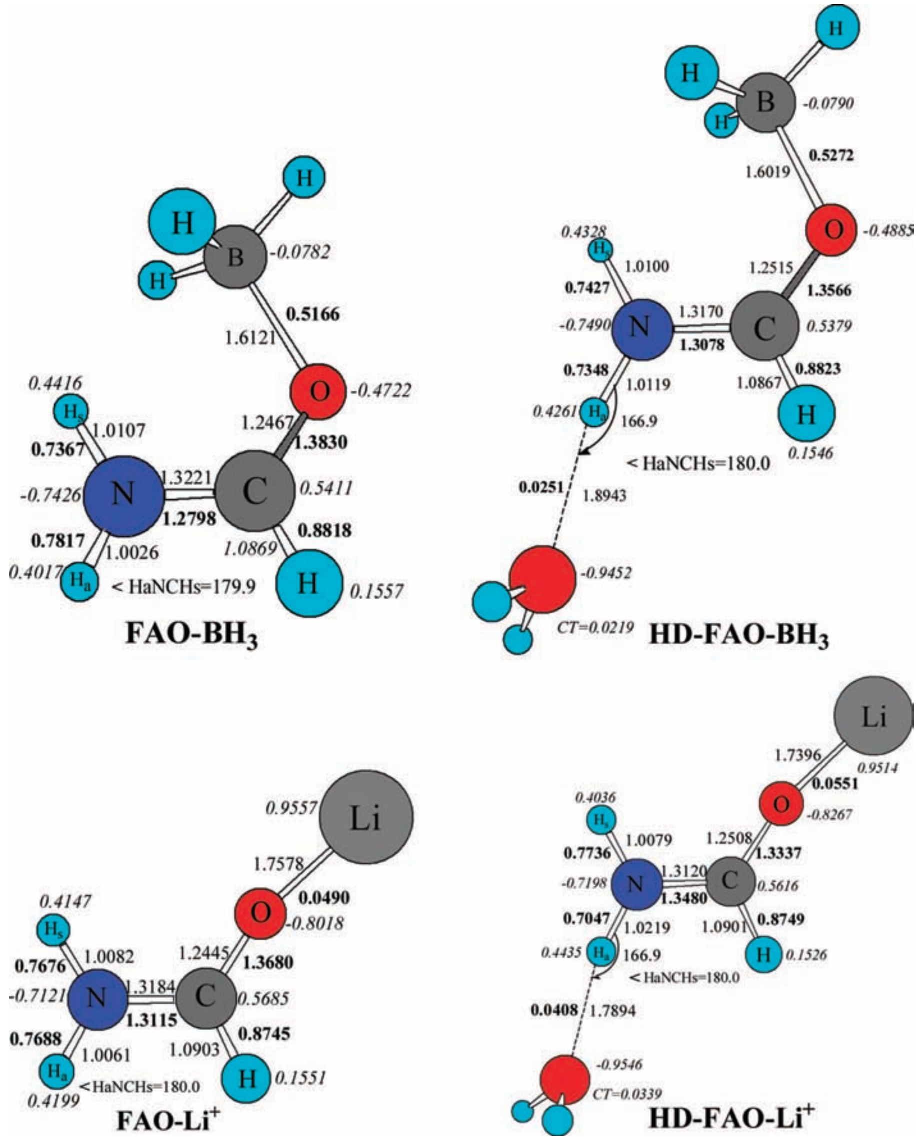

Figure 8. MP2/cc-pVTZ geometries of **FAO-BH$_3$**, **HD-FAO-BH$_3$, FAO-Li$^+$**, **HD-FAO-Li$^+$** (bond lengths in angstroms, bond and dihedral angles in degrees), MP2/aug-cc-pVTZ//MP2/cc-pVTZ natural charges (in e) in italic, and MP2/aug-cc-pVTZ//MP2/cc-pVTZ WBIs in bold.

4. Conclusions

By using formamide, its derivatives, and their H-bonded complexes with water as models, we have performed ab initio calculations up to MP2/aug-cc-pVTZ//MP2/cc-pVTZ to study the two-way effects between the intramolecular resonance effect and H-bond. It has been shown that the resonance effect influences not only the H-bond strength but also the type. Unlike NH_3 and NH_2CH_3 which prefer being **HAs**, the amino groups in the six monomers can all serve as **HDs**, and only two monomers (**FAC** and **FASi**) can serve as **HA** to form stable H-bonded complexes with water. The NRT analyses and the N−C bond contractions indicate that the resonance effect strengthens **HD** and weakens **HA** H-bonds. In reverse, the **HD** H-bonds also enhance the resonance effect, and **HA** H-bond weakens it. The H-bond energies in the **FAC-, FAN-**, **FAO-**, **FASi-**, **FAP-**, and **FAS-HD** complexes, −2.22, −2.90, −3.30, −2.52, −3.48, −3.95 kcal/mol, respectively, are well correlated with the weights of the π resonance (8.2, 10.6, 27.3, 10.8, 20.0, and 29.4%, respectively) and the N−C bond lengths (1.3937, 1.3730, 1.3576, 1.3853, 1.3663, and 1.3433 Å, respectively). The two-way effects can also be observed in the **HA$_{co}$**-type complex in which **FAO** oxygen serves as **HA**.

The two-way effects are cooperative. Because the **HD** and **HA$_{co}$** H-bonds are present simultaneously, the resonance effect is enhanced, and the H-bond energy increases much more significantly than in the case when only one H-bond is present.

The two-way effects can be explained as follows: the resonance effect influences the intramolecular charge population which facilitates or prevents the charge donation or acceptation with their H-bond partners and therefore strengthens or weakens the H-bonds. In reverse, the intermolecular charge donation or acceptation with H-bond partners facilitates or prevents the intramolecular charge shifts in the monomer, which enhances or weakens the resonance effect.

By using the knowledge about the two-way effects, as an example, we computationally designed **FAO-BH$_3$**. Because of the electron donation of carbonyl group to empty π orbital of BH_3, the resonance effect in **FAO-BH$_3$** is enhanced significantly, relative to **FAO**. Owing to the enhanced resonance effect, the H-bond energy in the **HD-FAO-BH$_3$**, −5.55 kcal/mol, is much larger that in the **FAO-HD** complex (−3.30 kcal/mol).

We have found no contradictions to Pauling's resonance model. Although we have not provided direct evidence against Wiberg and co-worker's resonance model, the various good correlations support Glendening and Harbal's opinion that an orbital-based NPA analysis may be more appropriate than a coordinate-based AIM analysis.

The understanding to the two-way effects may be helpful in drug design and refinement and in building empirical H-bond models for simulating large biological molecules.

Acknowledgment. Supports in China by NSFC(20773160) to Z.X.W. and NSFC (20773161) to M.B.H. and in the U.S. by NIH (GM64458) to Y.D. are acknowledged.

Supporting Information Available: MP2/aug-cc-pVTZ//MP2/cc-pVTZ potential energy surface of formamide by using N−C and C−O bond lengths as reaction coordinates (SI1). Geometries of **FAN-HA** complex optimized at MP2/6-31G**, MP2/6-311+G**, and MP2/cc-pVTZ (SI2). This material is available free of charge via Internet at http://pubs.acs.org.

References and Notes

(1) Greenberg, A.; Breneman, C. M.; Liebman, J. F. *The Amide Linkage: Structural Significance in Chemistry, Biochemistry, and Materials Science*; Willy: New York, 2000.

(2) Greenberg, A.; Breneman, C. M.; Liebman, J. F. *The Amide Linkage: Structural Significance in Chemistry, Biochemistry, and Materials Science*; Willy: New York, 2002.

(3) Boyd, D. B. *J. Med. Chem.* **1993**, *36*, 1443.

(4) Jungheim, L. N.; Boyd, D. B.; Indelicato, J. M.; Pasini, C. E.; Preston, D. E.; Alborn, W. E., Jr *J. Med. Chem.* **1991**, *34*, 1732.

(5) Kurland, R. J.; Wilson, E. B., Jr *J. Chem. Phys.* **1957**, *27*, 585.

(6) Costain, C. C.; Dowling, J. M. *J. Chem. Phys.* **1960**, *32*, 158.

(7) Kamei, H. *Bull. Chem. Soc. Jpn.* **1968**, *41*, 2269.

(8) Christensen, D. H.; Kortzeborn, R. N.; Bak, B.; Led, J. J. *J. Chem. Phys.* **1970**, *53*, 3912.

(9) Drakenberg, T.; Forsen, S. J. *Phys. Chem.* **1970**, *74*, 1.

(10) Perricaudet, M.; Pullman, A. *J. Pept. Protein Res.* **1973**, *5*, 99.

(11) Hirota, E.; Sugisaki, R.; Nielsen, C. J.; Sørensen, G. O. *J. Mol. Spectrosc.* **1974**, *49*, 251.

(12) Harding, L. B.; Goddard, W. A., III *J. Am. Chem. Soc.* **1975**, *97*, 6300.

(13) Nalewajski, R. F. *J. Am. Chem. Soc.* **1978**, *100*, 41.

(14) Carlsen, N. R.; Radom, L.; Riggs, N. V.; Rodwell, W. R. *J. Am. Chem. Soc.* **1979**, *101*, 2233.

(15) Fogarasi, G.; Pulay, P.; Török, F.; Boggs, J. E. *J. Mol. Struct.* **1979**, *57*, 259.

(16) Hansen, E. L.; Larsen, N. W.; Nicolaisen, F. M. *Chem. Phys. Lett.* **1980**, *69*, 327.

(17) Radom, L.; Riggs, N. V. *Aust. J. Chem.* **1980**, *33*, 249.

(18) Williams, J. O.; van Alsenoy, C.; Schäfer, L. *J. Mol. Struct. (THEOCHEM)* **1981**, *76*, 171.

(19) Chan, B.; Shukla, J. P.; Walker, S. *J. Mol. Struct.* **1983**, *102*, 165.

(20) Boggs, J. E.; Niu, Z. J. *Comput. Chem.* **1985**, *6*, 46.

(21) Jasien, P. G.; Stevens, W. J.; Krauss, M. *J. Mol. Struct. (THEOCHEM)* **1986**, *139*, 197.

(22) Brown, R. D.; Godfrey, P. D.; Kleibömer, B. *J. Mol. Spectrosc.* **1987**, *124*, 34.

(23) Wiberg, K. B.; Laidig, K. E. *J. Am. Chem. Soc.* **1987**, *109*, 5935.

(24) Wang, X.-C.; Nichols, J.; Feyereisen, M.; Gutowski, M.; Boatz, J.; Haymet, A. D. J.; Simons, J. *J. Phys. Chem.* **1991**, *95*, 10419.

(25) Burton, N. A.; Chiu, S. S.-L.; Davidson, M. M.; Green, D. V. S.; Hillier, I. H.; McDouall, J. J.; Vincent, M. A. *J. Chem. Soc., Faraday Trans.* **1993**, *89*, 2631.

(26) Dixon, D. A.; Matsuzawa, N. *J. Phys. Chem.* **1994**, *98*, 3967.

(27) Olson, L. F.; Li, Y.; Houk, K. N.; Kresge, A. J.; Schaad, L. J. *J. Am. Chem. Soc.* **1995**, *117*, 2992.

(28) Fogarasi, G.; Szalay, P. G. *J. Phys. Chem. A* **1997**, *101*, 1400.

(29) Demaison, J.; Császár, A. G.; Kleiner, I.; Møllendal, H. J. *Phys. Chem. A* **2007**, *111*, 2574.

(30) Glendening, E. D.; Hrabal, J. A. *J. Am. Chem. Soc.* **1997**, *119*, 12940.

(31) Mo, Y.; Schleyer, P. v. R.; Wu, W.; Lin, M.; Zhang, Q.; Gao, J. *J. Phys. Chem. A* **2003**, *107*, 10011.

(32) Mo, Y. *J. Chem. Phys.* **2003**, *119*, 1300.

(33) Lauvergnat, D.; Hiberty, P. C. *J. Am. Chem. Soc.* **1997**, *119*, 9478.

(34) Wiberg, K. B. *Acc. Chem. Res.* **1999**, *32*, 922.

(35) Wiberg, K. B.; Breneman, C. M. *J. Am. Chem. Soc.* **1992**, *114*, 831.

(36) Wiberg, K. B.; Hadad, C. M.; Rablen, P. R.; Cioslowski, J. *J. Am. Chem. Soc.* **1992**, *114*, 8644.

(37) Wiberg, K. B.; Rablen, P. R. *J. Am. Chem. Soc.* **1995**, *117*, 2201.

(38) Pauling, L. *The Nature of the Chemical Bond*, 3rd ed.; Cornell University: Ithaca, NY, 1960.

(39) Beck, J. F.; Mo, Y. *J. Comput. Chem.* **2007**, *28*, 455.

(40) Gilli, G.; Bellucci, F.; Ferretti, V.; Bertolasi, V. *J. Am. Chem. Soc.* **1989**, *111*, 1023.

(41) Bingham, A. H.; Davenport, R. J.; Gowers, L.; Knight, R. L.; Lowe, C.; Owen, D. A.; Parry, D. M.; Pitt, W. R. *Bioorg. Med. Chem. Lett.* **2004**, *14*, 409.

(42) Hao, M.-H. *J. Chem. Theory Comput.* **2006**, *2*, 863.

(43) Boys, S. F.; Bernardi, F. *Mol. Phys.* **1970**, *19*, 553.

(44) Frisch, M. J.; Trucks, G. W.; Schlegel, H. B.; Scuseria, G. E.; Robb, M. A.; Cheeseman, J. R.; Montgomery, J. A., Jr.; Vreven, T.; Kudin, K. N.; Burant, J. C.; Millam, J. M.; Iyengar, S. S.; Tomasi, J.; Barone, V.; Mennucci, B.; Cossi, M.; Scalmani, G.; Rega, N.; Petersson, G. A.; Nakatsuji, H.; Hada, M.; Ehara, M.; Toyota, K.; Fukuda, R.; Hasegawa, J.; Ishida, M.; Nakajima, T.; Honda, Y.; Kitao, O.; Nakai, H.; Klene, M.; Li, X.; Knox, J. E.; Hratchian, H. P.; Cross, J. B.; Bakken, V.; Adamo, C.; Jaramillo, J.; Gomperts, R.; Stratmann, R. E.; Yazyev, O.; Austin, A. J.; Cammi, R.; Pomelli, C.; Ochterski, J. W.; Ayala, P. Y.; Morokuma, K.; Voth, G. A.; Salvador, P.; Dannenberg, J. J.; Zakrzewski, V. G.; Dapprich, S.; Daniels, A. D.; Strain, M. C.; Farkas, O.; Malick, D. K.; Rabuck, A. D.; Raghavachari, K.; Foresman, J. B.; Ortiz, J. V.; Cui, Q.; Baboul, A. G.; Clifford, S.; Cioslowski, J.; Stefanov, B. B.; Liu, G.; Liashenko, A.; Piskorz, P.; Komaromi, I.; Martin, R. L.; Fox, D. J.; Keith, T.; Al-Laham, M. A.; Peng, C. Y.; Nanayakkara, A.; Challacombe, M.; Gill, P. M. W.; Johnson, B.; Chen, W.; Wong, M. W.; Gonzalez, C.; Pople, J. A. *Gaussian 03*, revision B.04; Gaussian, Inc.: Wallingford, CT, 2003.

(45) Florián, J.; Johnson, B. G. *J. Phys. Chem.* **1994**, *98*, 3681.

(46) Ruiz, E.; Salahub, D. R.; Vela, A. *J. Phys. Chem.* **1996**, *100*, 12265.

(47) Zhao, Y.; Truhlar, D. G. *J. Phys. Chem. A* **2005**, *109*, 6624.

(48) Zhao, Y.; Truhlar, D. G. *J. Chem. Theory Comput.* **2005**, *1*, 415.

(49) Reed, A. E.; Weinhold, F. *J. Chem. Phys.* **1983**, *78*, 4066.

(50) Reed, A. E.; Weinstock, R. B.; Weinhold, F. *J. Chem. Phys.* **1985**, *83*, 735.

(51) Weinhold, F.; Carpenter, J. E. In *The Structure of Small Molecules and Ions*; Naaman, R., Vager, Z., Eds.; Plenum: New York, 1988; 227−236.

(52) Glendening, E. D.; Weinhold, F. *J. Comput. Chem.* **1998**, *19*, 593.

(53) Glendening, E. D.; Weinhold, F. *J. Comput. Chem.* **1998**, *19*, 610.

(54) Glendening, E. D.; Badenhoop, J. K.; Weinhold, F. *J. Comput. Chem.* **1998**, *19*, 628.

(55) Wiberg, K. B. *Tetrahedron* **1968**, *24*, 1083.

(56) Glendening, E. D.; Badenhoop, J. K.; Reed, A. E.; Carpenter, J. E.; Bohmann, J. A.; Morales, C. M.; Weinhold, F. *NBO. 5.0*; Theoretical Chemistry Institute, University of Wisconsin, Madison, WI, 2001.

(57) Mo, Y.; Schleyer, P. v. R. *Chem. Eur. J.* **2006**, *12*, 2009.

(58) Delley, B. *J. Chem. Phys.* **1991**, *94*, 7245.

(59) Weinhold, F. Natural bond orbital methods In *Encyclopedia of computational chemistry*; Schleyer, P. v. R. Ed.; Wiley: New York, 1998; Vol. 3, 1792−1811.

(60) Scheiner, S. *Hydrogen Bonding*; Oxford University Press: New York, 1997.

(61) Desiraju, G. R.; Steiner, T. *The Weak Hydrogen Bond*; Oxford University Press: Oxford, 1999.

(62) Dykstra, C. E. *Acc. Chem. Res.* **1988**, *21*, 355.

(63) Reed, A. E.; Curtiss, L. A.; Weinhold, F. *Chem. Rev.* **1988**, *88*, 899.

(64) Wu, Y. D.; Zhao, Y. L. *J. Am. Chem. Soc.* **2001**, *123*, 5313.

(65) Zhao, Y. L.; Wu, Y. D. *J. Am. Chem. Soc.* **2002**, *124*, 1570.

(66) Ludwig, R. *J. Mol. Liq.* **2000**, *84*, 65.

(67) Ludwig, R.; Reis, O.; Winter, R.; Weinhold, F.; Farar, T. C. *J. Phys. Chem. B* **1998**, *102*, 9312.

(68) Ludwig, R.; Weinhold, F.; Farrar, T. C. *J. Phys. Chem. A* **1997**, *101*, 8861.

(69) Kobko, N.; Paraskevas, L.; delRio, E.; Dannenberg, J. J. *J. Am. Chem. Soc.* **2001**, *123*, 4348.

(70) Masunov, A.; Dannenberg, J. J. *J. Phys. Chem. B.* **2000**, *104*, 806.

(71) Guo, H.; Gresh, N.; Roques, B. P.; Salahub, D. R. *J. Phys. Chem. B.* **2000**, *104*, 9746.

(72) Guo, H.; Salahub, D. R. *Angew. Chem., Int. Ed.* **1998**, *37*, 2985.

(73) Guo, H.; Karplus, M. *J. Phys. Chem.* **1994**, *98*, 7104.

(74) Chen, Y. F.; Dannenberg, J. J. *J. Am. Chem. Soc.* **2006**, *128*, 8100.

(75) Salvador, P.; Kobko, N.; Wieczorek, R.; Dannenberg, J. J. *J. Am. Chem. Soc.* **2004**, *126*, 14190.

(76) Viswanathan, R.; Asensio, A.; Dannenberg, J. J. *J. Phys. Chem. A* **2004**, *108*, 9205.

(77) Kobko, N.; Dannenberg, J. J. *J. Phys. Chem. A* **2003**, *107*, 10389.

JP712052E